

Unusual Surface Aging of Poly(dimethylsiloxane) Elastomers

Anish Kurian,[†] Shishir Prasad,^{†,‡} and Ali Dhinojwala^{*,†}

[†]Department of Polymer Science, The University of Akron, Akron, Ohio 44325-3909, and [‡]Universal Technology Corporation, Dayton, Ohio 44325-3909

Received November 27, 2009; Revised Manuscript Received January 5, 2010

ABSTRACT: We have observed an unusual increase in adhesion hysteresis and frictional forces for poly(dimethylsiloxane) (PDMS) lenses sliding on smooth glassy surfaces after a period of aging in a laboratory environment. X-ray photoelectron spectroscopy, contact angle, and in situ surface-sensitive sum frequency generation spectroscopy (SFG) measurements show no differences between an aged and unaged lens, indicating that these changes in tribological properties cannot be due to surface contaminant or degradation. Instead, we observed that the SFG intensity of the PDMS Si–CH₃ symmetric band is 3 orders of magnitude higher after sliding the aged lenses. Such a large increase in the SFG signal can only arise from very well-ordered PDMS molecules induced by sliding and has important consequences in understanding adhesion hysteresis and friction.

1. Introduction

Poly(dimethylsiloxane) (PDMS) is widely used as a model elastomer to study adhesion and friction.^{1–4} Because of the robustness of the platinum catalyst used for cross-linking, hydrophobicity, transparency, and nanometer-smooth surfaces, PDMS is used in the areas of soft lithography, release coating, biomaterial, and medical implants.^{5–8} In our experiments on friction and adhesion of PDMS lenses in contact with glassy methacrylate polymers, we have observed an unusually high adhesion hysteresis and friction for PDMS lenses that were stored for an extended period of time (aged lenses) as compared to the lenses that were prepared and used within a week (fresh lenses). This effect was very reproducible, and we could not explain these results based on the lenses being contaminated during storage or due to the generation and segregation of short oligomeric PDMS chains upon aging. Additionally, we did not observe any differences between the aged and fresh samples using X-ray photoelectron spectroscopy (XPS) and contact angle measurements.

To understand the effect of aging, we have studied the contact interface between PDMS lenses and poly(*n*-propyl methacrylate) (PPMA)-coated sapphire prisms using the surface-sensitive infrared visible sum frequency generation (SFG) spectroscopy in total internal reflection geometry. According to the dipole approximation, the generation of SFG photons is forbidden in centrosymmetric bulk and permitted only at interfaces where the inversion symmetry is broken.⁹ The surface selectivity of SFG is important in probing the interfacial structure without the measurements being swamped by the signals generated in the bulk, which is a common problem encountered in using Raman and IR techniques. Additionally, the SFG conversion is resonantly enhanced when the infrared frequency overlaps with the molecular–vibrational modes that are both Raman- and infrared-active. The position and the magnitude of these resonance peaks provide chemical and orientation information on the molecules at the buried interface. On the basis of molecular dynamics simulations on polystyrene and PDMS,^{10,11} we estimate that SFG is probing a 5–10 Å thick interfacial layer.

We have observed no differences between the aged and unaged lenses at the PDMS/PPMA interface in static contact using SFG, even though there were striking differences in adhesion and

friction properties. Interestingly, the biggest differences were observed only after sliding PDMS lenses on the PPMA-coated surface. The SFG intensity of the PDMS Si–CH₃ symmetric peak increases by almost 3 orders of magnitude upon sliding the aged lens on the PPMA. This dramatic increase in SFG signal can only be due to alignment of PDMS chains at the contact interface. These measurements were conducted on aged lenses after extracting them in toluene to remove the short oligomeric chains, and this rules out possibilities of short oligomeric chains due to hydrolysis affecting the SFG results. The near identical surface nature of the aged and unaged lenses suggests that the differences due to aging are very subtle and indistinguishable in a static contact. We suggest that aging results in chain scission which disrupts the cross-linking and increases the density of the surface anchored chains with one free end. These surface anchored chains are stretched during sliding as postulated by the earlier theories in the area of rubber friction by Schallamach.¹² We postulate that the stretching of chains also leads to ordering of these molecules at the interface. Interestingly, the ordering is not permanent, and the surface structure relaxes after we stop sliding. These relaxation time constants are much higher than those expected based on bulk viscosity. Although we started out to understand the differences due to aging, we have made the first direct observation of orientation of molecules during sliding, which was expected but not experimentally observed before.

2. Experimental Section

2.1. Sample Preparation. PDMS lenses were made by mixing a desired amount of divinyl-terminated PDMS ($M_w \approx 6000$ g/mol) with 10% cross-linker (25–30% methylhydrosiloxane–dimethylsiloxane copolymer, $M_w \approx 1950$ g/mol) and 3% catalyst (platinum–cyclovinylmethylsiloxane complex). All materials were obtained from Gelest Inc. and were used as received. The mixture was left for an hour after thorough mixing to remove the entrapped air. Hemispherical lenses were prepared by placing small droplets of the mixture onto fluorinated glass slides and subsequently curing in an oven for 4 h at 60 °C. Flat sheets of ~1 mm thickness for XPS experiments were obtained by casting the mixture in an Al dish. The un-cross-linked residue in PDMS lenses was removed by placing the cured lenses in a beaker lined with filter paper and extracting in excess amount of toluene for 2 weeks. The solvent was changed at regular intervals for 4–5 times. The extracted lenses were finally dried overnight

*Corresponding author. E-mail: ali4@uakron.edu.

at room temperature followed by overnight drying under vacuum at 60 °C. Some selected lenses were also heated to 140 °C for 6 h to ensure that the annealing procedure was sufficient to remove the residual toluene. No differences in the SFG results were observed upon additional annealing, and we report here the results without this extra heating step. These fresh lenses were stored in a Petri dish at room condition (20–25 °C and 40–60% relative humidity) for a time period of 2–24 months for aging study. The postcuring procedure for PDMS sheets was same as PDMS lenses. The roughness of the lenses was 0.5 nm as measured using AFM.

The counter PPMA (Scientific Polymer Products, Inc., $M_w \approx 250K$ g/mol, $T_g = 35$ °C) surface was prepared by spin-coating 2 wt % solution in toluene at 2000 rpm on a clean sapphire prism. The films were annealed in a vacuum oven at 45 °C for 4 h. The PPMA films were ≈ 300 nm in thickness (measured using ellipsometer).

2.2. Friction and Adhesion Measurements. Friction and adhesion measurements were performed at room condition using a custom-built instrument consisting of two perpendicular bridge assembly to measure shear and normal forces.¹³ The capacitance sensors, attached to the bridges, were used to measure displacement. The spring constants of the bridges were calibrated by hanging known weights and measuring displacement. PDMS lenses were brought into contact with the PPMA-coated sapphire prism mounted on a holder. Friction experiments were conducted using high-resolution picometer motors at a relative velocity of 0.1–60 $\mu\text{m/s}$ and a normal load of 300 mg. The contact area during the experiments was measured using a Olympus DP25 camera.

The adhesion measurements were performed using the Johnson–Kendall–Roberts (JKR) geometry.¹⁴ We measured the contact area of a hemispherical lens in contact with a flat substrate as a function of loading (adhesion) and unloading (fracture).¹⁵ The energy release rate, G , was calculated using the equation

$$a^3 = \frac{R}{K} \left[P + 3\pi RG + \sqrt{6\pi RGP + (3\pi RG)^2} \right] \quad (1)$$

where a is the contact radius, R is the radius of curvature of the lens, P is the applied load, and K is the elastic constant of the system. R was determined by imaging the contact lens side ways. The adhesion measurements were conducted by changing the normal load in steps of 500 μN at 5 min intervals. We can also express the JKR equation in the form of $G = (Ka^3/R - P)^2/6\pi Ka^3$.¹⁶ In an ideal situation, where there are no other dissipative processes, G = the true thermodynamic work of adhesion, W_a . However, in many instances there are nonequilibrium processes such as interdigitation, disentanglements, inelastic deformation, and restructuring at interfaces which result in G less than the thermodynamic work of adhesion during loading and G being greater than the thermodynamic value during unloading² (or adhesion hysteresis).

2.3. X-ray Photoelectron Spectroscopy. XPS was performed on fresh and aged PDMS lenses using Kratos AXIS Ultra DLD. The Al monochromator was used as the X-ray source. Charge neutralization was used to prevent charging of the samples. In addition, we have shifted the peak using the reference of C 1s peak which is supposed to be at 284.5 eV. The elemental surface composition (X_i 's) of the sample can be obtained by normalizing the peak area (A_i) corresponding to each element ($j = 1$ to n) with their respective relative sensitivity factor (RSF_{*j*}) and using the following equation:¹⁷

$$X_i = \frac{\frac{A_i}{\text{RSF}_i}}{\sum_{j=1}^n \frac{A_j}{\text{RSF}_j}} \quad (2)$$

Here, $\sum_{j=1}^n X_j = 1$ excluding hydrogen in our case (XPS cannot detect hydrogen and helium).

2.4. Sum Frequency Generation Spectroscopy. SFG is a second-order nonlinear spectroscopic technique which is useful for nondestructive analysis of surfaces or interfaces. The details of this technique have been explained elsewhere.^{18,19} Briefly, SFG involves the spatial and temporal overlap of a high-intensity visible laser beam of frequency ω_{vis} with a tunable infrared beam of frequency ω_{IR} to generate a second-order beam of frequency ($\omega_{\text{vis}} + \omega_{\text{IR}}$). According to the dipole approximation, the generation of the SFG photons is forbidden in the centrosymmetric bulk and permitted only at the surface or interface where the symmetry is broken. The sum frequency signal is resonantly enhanced when ω_{IR} overlaps with the molecular vibration mode of the asymmetric surface or interface molecules. Hence, a SFG spectrum provides information regarding the chemical groups present at the surface. In addition, the relative magnitude of different vibrations from a chemical group is decided by its orientation.^{10,20–22} In addition, the total internal reflection (TIR) geometry enhances the SFG intensity by ~ 2 orders of magnitude. We have used the TIR geometry to selectively probe the interface of interest (PDMS/PPMA) by the proper choice of incident angle.

SFG spectra were acquired at room condition using a pico-second laser system (Spectra-Physics) with a tunable IR beam (2000–3800 cm^{-1} , 1 ps pulse width, 1 kHz repetition rate, and a diameter of 100–200 μm) and a visible beam (800 nm, 1 ps pulse width, 1 kHz repetition rate, and a diameter of 1 mm). Spectra were acquired in SSP (S polarized SFG, S polarized red, and P polarized IR) polarization combination. The acquired spectra were normalized by the power of the infrared beam and fitted using a Lorentzian equation

$$I_{\text{SFG}} \propto \left| \chi_{\text{eff,NR}} + \sum_q \frac{A_q e^{i\phi_q}}{\omega_{\text{IR}} - \omega_q - i\Gamma_q} \right|^2 \quad (3)$$

where A_q , Γ_q , ω_q , and ϕ_q are the strength, damping constant, angular frequency, and phase of a resonant vibration, respectively. $\chi_{\text{eff,NR}}$ is the nonresonant part of the SFG signal.

Incident angles of 42° and 12° were used to collect SFG spectra for polymer/air and the PDMS/PPMA interfaces, respectively. The contact spectra were gathered after bringing the PDMS into contact with the PPMA substrate. After this step, the lens was retracted and brought into contact behind the laser spot. The lens was then moved toward the laser spot with a constant velocity. When the contact spot overlapped with the incident laser, the motor was stopped and the SFG spectra were collected immediately.

3. Results and Discussion

3.1. Friction and Adhesion at PDMS/PPMA Interface.

Figure 1A shows the shear stress as a function of sliding velocity for fresh and 18-month-aged PDMS lenses sliding on PPMA surface. The shear stress for aged lenses is significantly higher than fresh lenses, and the difference is more pronounced at a higher sliding velocity. These differences between the aged and fresh lenses were also observed in adhesion experiments. In Figure 1B,C we have shown the changes in contact radius as a function of applied load in both loading and unloading cycles for the fresh and aged lenses, respectively. The modulus of the lens and G can be calculated by fitting the data using the JKR equation (eq 1). We obtain the same modulus for both fresh and aged lenses (~ 1.1 MPa). The G_l (during loading) and G_{ul} (during unloading) values for fresh lens are 49 ± 1 mJ/m^2 and 49 ± 2 mJ/m^2 . For aged lens, the G_l and G_{ul} values are 42 ± 1 mJ/m^2 and 57 ± 3 mJ/m^2 , respectively. The adhesion hysteresis for fresh lenses is ≈ 0 and 15 mJ/m^2 for aged lenses. Lower G_l

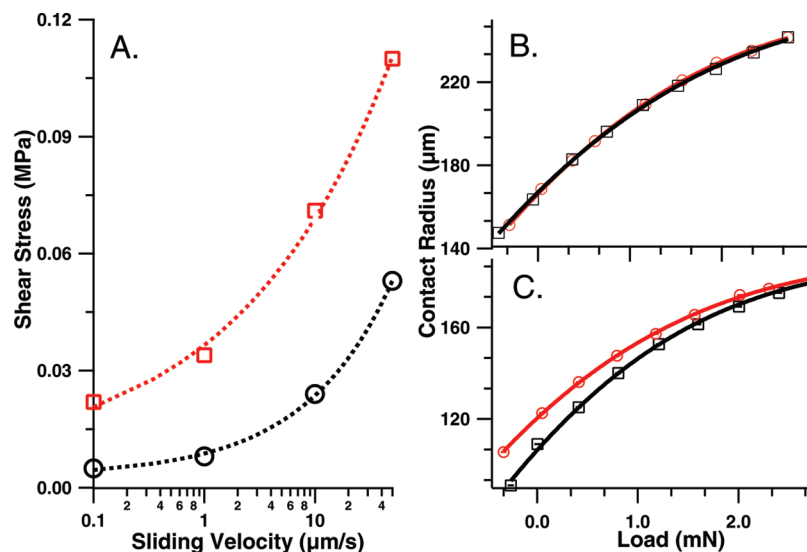


Figure 1. (A) Shear stress as a function of sliding velocity for fresh (○) and 18-month-aged (□) PDMS lenses sliding on the PPMA surface. (B) Fresh PDMS and (C) aged PDMS represent the contact radius in JKR adhesion measurements as a function of normal load in the loading (□) and unloading (○) cycles for the interfaces in (A).

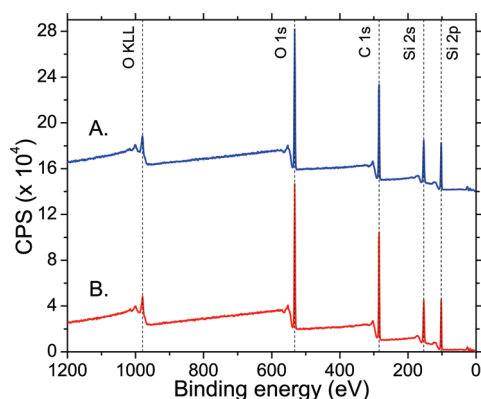


Figure 2. Counts per second (CPS) as a function of binding energy of photoelectron obtained using XPS on fresh (A) and 12-month-aged (B) PDMS sheets. The data were normalized by C 1s peak position (284.5 eV) to compensate for the sample charging.

and higher G_{ul} for aged lenses compared to $W_a \approx 49 \text{ mJ/m}^2$ is expected for systems exhibiting hysteresis.²

The similarity in the modulus for aged and unaged lenses indicates that there is no significant cross-linking or degradation of bulk PDMS structure during aging. Hence, the higher adhesion hysteresis and friction for aged lenses can be attributed to the modification of the PDMS surface (or near surface region) with aging. To rule out the surface contamination and chemical changes as reasons, we have performed XPS measurements on fresh and 12-month-aged PDMS (Figure 2). The peak positions marked in Figure 2 correspond to elements we expect for PDMS.²³ The RSF, peak area, and surface composition (determined using eq 2) are provided in Table 1. The surface composition for fresh and aged PDMS samples is similar and matches with values expected for PDMS (C:O:Si::2:1:1). In addition, we have collected high-resolution XPS scans in the oxygen, silicon, and carbon regions. No additional broadening or shoulder peaks were observed for fresh and aged PDMS samples.

It is also possible that aging results in generation and migration of short oligomeric PDMS chains to the surface or interface. The experimental results for aged PDMS samples reported here were collected after extracting the lenses in toluene. The

Table 1. Peak Analysis of the XPS Spectra Shown in Figure 2^a

element	RSF	A_{fresh}	A_{aged}	X_{fresh}	X_{aged}
C	0.278	8500 ± 100	9100 ± 300	53	55
O	0.780	11300 ± 200	11200 ± 500	25	24
Si	0.328	4100 ± 100	4000 ± 100	22	21

^a RSF, peak area (A), and the calculated elemental composition (X , at. %) for fresh and 12-month-aged PDMS lenses are tabulated.

extraction process is expected to remove low molecular weight PDMS chains. Therefore, we rule out the possibility of loose chains causing the differences in friction or adhesion. Because XPS can only be used in vacuum, the possibility of detecting differences between the fresh and aged PDMS lenses after contact with PPMA is not feasible. To understand the striking differences in friction and adhesion, we have taken the advantage of the sensitivity of the SFG technique to directly probe the buried interface between PDMS and PPMA.

3.2. Probing Static and Dynamic PDMS/PPMA Interface Using SFG. Parts A and C of Figure 3 show the SFG spectra in SSP polarization of fresh and 18-month-aged PDMS lenses in contact with the PPMA surface, respectively. The solid lines are the fits to the data using eq 3. From the fits we determine that the prominent peaks in the spectra are assigned to PPMA (CH_3 symmetric (r^+ , 2880 cm^{-1}), CH_3 Fermi (2940 cm^{-1}), and CH_3 asymmetric (r^- , 2955 cm^{-1})). The Si- CH_3 peaks for PDMS if present would be at 2910 and 2965 cm^{-1} . We find similar A_q values for fresh and aged PDMS lenses, suggesting that the SFG spectra are indistinguishable. The SFG and XPS data exclude the possibility of surface contamination of aged PDMS lenses as the reason for observed differences in the friction and adhesion experiments (Figure 1).

The SFG spectra obtained after sliding the fresh and aged (aged for 4, 8, and 18 months) PDMS lenses at $50 \mu\text{m/s}$ in contact with PPMA are shown in parts B and D of Figure 3, respectively. The data are fitted using eq 3 (solid lines in the figures). In the case of the fresh lens, the spectra obtained in static contact (Figure 3A) and after sliding (Figure 3B) are similar, suggesting that no observable changes are taking place at the interface as a result of sliding. In contrast, significant differences are observed between the two spectra (Figure 3C,D) for aged PDMS lenses obtained before and after sliding. After sliding, the SFG spectra have two

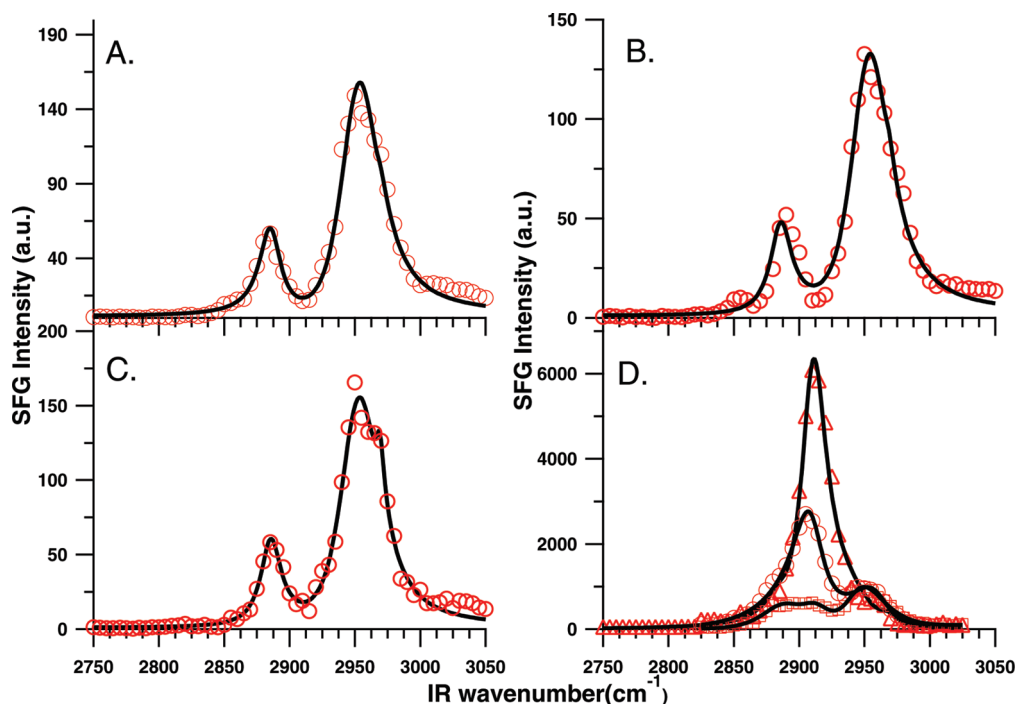


Figure 3. SFG spectra in SSP polarization of a fresh PDMS lens/PPMA interface in contact (A) and after sliding at 50 $\mu\text{m/s}$ (B). The spectrum remains unchanged for the fresh lens after the friction experiment. SFG spectra of aged lens/PPMA interface in contact (C, 18-month-aged lens) and after sliding at 50 $\mu\text{m/s}$ (D, aging time: 4 (\square), 8 (\circ), and 18 months (\triangle)). The data for 4 and 8 months in (D) are multiplied by a factor of 7 for illustrating the changes in the spectral features. The solid lines are the fits to the data using eq 3. Significant enhancement in 2910 cm^{-1} peak, as a function of aging time, is observed upon sliding of the aged PDMS lens.

additional peaks at 2910 and 2965 cm^{-1} corresponding to the Si-CH₃ symmetric and Si-CH₃ asymmetric bands, respectively. The intensity of the Si-CH₃ symmetric peak increases with aging, suggesting that the changes at the interface continue to evolve with aging time. On the other hand, we have observed no differences in the PPMA structure on sliding fresh or aged PDMS lenses. We have observed similar results for PDMS lenses in contact with poly(ethyl methacrylate) ($T_g = 65^\circ\text{C}$) films, indicating that the low T_g of PPMA ($= 35^\circ\text{C}$) is not the reason for the changes observed during sliding. These large increases in the SFG signal of PDMS can only be generated from surface species that are well ordered at the interface. It is puzzling how aging could result in strong ordering of PDMS molecules upon sliding.

Before we discuss the origin of this ordering, we have analyzed the orientation of PDMS molecules using the SFG data. The strong enhancement in the SFG signals observed in sliding is similar to the strong enhancement of the Si-CH₃ symmetric peak that was found for oxidized PDMS in static contact with a self-assembled monolayer (octadecyltrichlorosilane, OTS) by Yurdumakan et al.¹⁰ In this earlier study, on the basis of spectral analysis, it was concluded that well-ordered PDMS chains at the interface are responsible for the enhancement of the Si-CH₃ peak. We postulate that a similar ordering of PDMS surface chains occurs upon sliding the aged PDMS lens against the PPMA surface and results in a strong enhancement of the Si-CH₃ symmetric peak. We can quantify the orientation of the PDMS surface chains by analyzing the ratio of the symmetric to the asymmetric A_q values of Si-CH₃ (obtained by the fit of SFG spectra using eq 3) using the following relationship:²⁴

$$\left| \frac{A_{q, \text{asym}}}{A_{q, \text{sym}}} \right| = \left| \frac{2\beta_{\text{caa}}}{\beta_{\text{ccc}}} \frac{\langle \cos \theta \rangle - \langle \cos^3 \theta \rangle}{\langle \cos \theta \rangle (1+r) - \langle \cos^3 \theta \rangle (1-r)} \right| \quad (4)$$

where $r = \beta_{\text{aac}}/\beta_{\text{ccc}}$ (β 's are the molecular hyperpolarizabilities) and θ is the angle of the Si-CH₃ symmetry axis with respect to the surface normal. The angular brackets $\langle \rangle$ implies the average of tilt angles. We have used $r \approx 2.3$ and $\beta_{\text{caa}}/\beta_{\text{ccc}} \approx 1$ for our calculation.²² For the aged PDMS lens after sliding, we obtain $|A_{q, \text{asym}}/A_{q, \text{sym}}| \approx 0.1$ and $\langle \cos \theta \rangle \approx 0.95$. The high value of $\langle \cos \theta \rangle$ indicates that the CH₃ group of PDMS preferentially orients perpendicular to the surface, and the surface chains are lying flat on the surface upon sliding.¹⁰

In the case of plasma-treated PDMS in contact with OTS monolayer, the orientation in static contact was due to the generation of short PDMS chains that are ordered in contact with the methyl groups of the OTS layer. We have used PDMS lenses that have been extracted in toluene to remove any low molecular weight PDMS chains in these experiments. Therefore, we can rule out the hypothesis of short chains migrating to the interface and being oriented due to sliding. Additionally, we have externally added low-viscosity PDMS short chains (~ 6000 g/mol) to a fresh PDMS lens and observed no changes in the SFG spectra during sliding, ruling out the possibility that the results we observed for aged lenses are due to short oligomeric PDMS chains. Interestingly, we also find very little evidence of PDMS chains being transferred to the PPMA surface after the sliding experiment. Parts A and B of Figure 4 show the SFG spectra in SSP polarization of the PPMA surface measured after the sliding experiment with a fresh and 18-month-aged PDMS lenses, respectively. Solid lines in the figures are the fits using eq 3. The two spectra are identical and are similar to the data obtained for PPMA surface before contact with PDMS lenses. This indicates that there is very little wear of PDMS lens during sliding. To confirm that SFG had the sensitivity to detect transfer of PDMS chains, we have measured the PPMA surface after sliding a plasma-treated PDMS lens and in that case we do observe significant transfer of PDMS material to the PPMA surface.

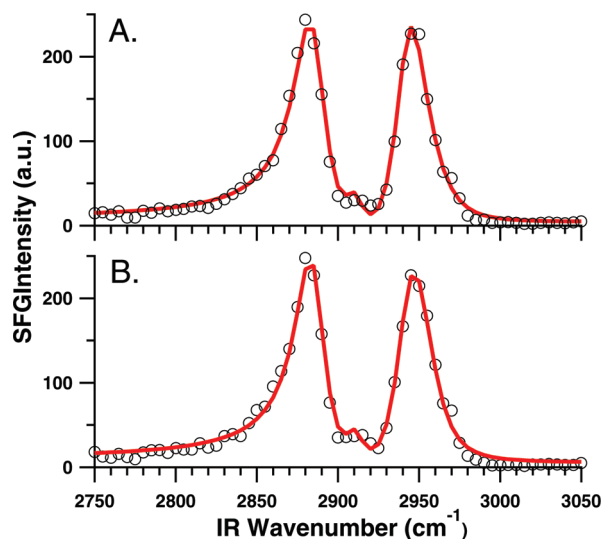


Figure 4. SFG spectra in SSP polarization of the PPMA surface after sliding against fresh (A) and 18-month-aged (B) PDMS lenses. The solid lines are the fits to the data using eq 3.

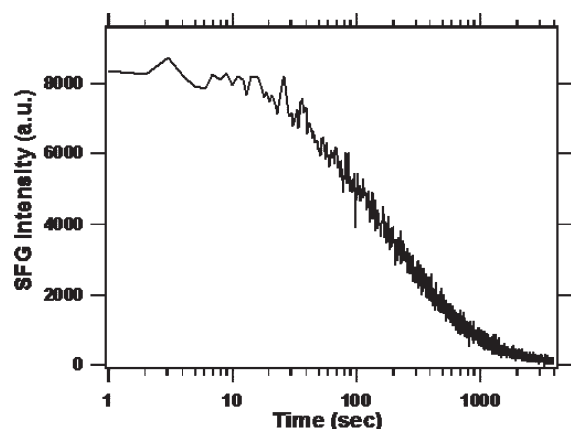


Figure 5. SFG intensity at 2910 cm^{-1} (Si-CH₃ symmetric peak) of 18-month-aged PDMS lens/PPMA interface as a function of time. The data were acquired after the sliding experiment (described in the Experimental Section) with time = 0 at the instance when the PDMS lens became stationary. SSP polarization combination was used for the measurements. It takes ≈ 1 h for the intensity to recover to the values for static contact (Figure 3C).

Interestingly, the enhancement in SFG intensity of Si-CH₃ symmetric peak upon sliding is not stable but slowly decays with time (Figure 5). The intensity data in Figure 5 were collected using SSP polarization and just after the PDMS lens overlapped with the laser spot. After an hour the SFG spectrum was similar to the SFG spectrum collected before sliding (Figure 3C). It is intriguing that the relaxation times are much longer than the relaxation time constant (in subsecond)²⁵ expected for the PDMS chains at these temperatures.

On the basis of the mechanical and spectroscopic results and prior observations reported in the literature, we propose a potential model to explain the differences in the results between the fresh and aged lenses. Using surface-tethered brushes, Brown¹ and Leger²⁶ have explained the increase in friction and adhesion by postulating that the brushes interpenetrate into the rubber network and the pulling-off of the chains requires additional energy that is reflected in an increase in adhesion and friction. Maeda et al.²⁷ have also explained the increase in adhesion and friction for ozone-

treated cross-linked polystyrene due to chain scission and formation of dangling chains that could penetrate into the cross-linked polystyrene substrate. Here, we propose that the aging results in chain scission and as a result dangling PDMS chains tethered by one end to the cross-linked PDMS network are created. The concept of tethering is important; otherwise, free chains would be transferred to the PPMA surface after sliding, which was not observed in these experiments (Figure 4). The dangling chains are then available to penetrate into the PPMA matrix, leading to an increase in the friction and adhesion forces.

These interfacial chains also show dynamics that are very slow compared to the PDMS chains in the bulk. Although the changes in the SFG spectra indicate significant ordering of the PDMS chains, we cannot determine what causes chain scission. We have tried to reproduce the effects of aging by exposing the PDMS surfaces to ozone or plasma (oxygen or nitrogen) treatments. Even though these surface treatments have a dramatic influence on the XPS and SFG results, we are unable to reproduce exactly the effects observed by aging the PDMS lenses.

Finally, we would like to reflect on why we did not observe any changes in the SFG spectra for fresh lenses upon sliding. There are two possibilities. First, the cross-linked PDMS structure prevents significant orientation of the PDMS chains. A second reason could be that the relaxation dynamics of these short cross-linked chains is much faster than that can be observed by the time resolution of the current SFG setup. Future experiments to understand the velocity and temperature dependence on the relaxation dynamics of these interfacial chains are in progress.

4. Conclusions

We have observed a very unusual increase in adhesion hysteresis and friction for PDMS lenses aged for a period of 4–18 months in contact with a glassy polymer, PPMA. The changes taking place at the surface of the PDMS surface due to aging were not differentiable with XPS and contact angle measurements. Interestingly, we could only observe the differences between the fresh and aged samples in the SFG spectra collected during sliding. The 3 orders of magnitude increase in the PDMS signals suggests significant ordering of the PDMS chains induced by sliding. The experimental evidence suggests that generation of surface dangling chains, and the interpenetration of these surface chains results in higher friction and adhesion hysteresis. Although these events have been anticipated based on force measurements, this is the first direct evidence of molecular orientation of interfacial molecules induced by sliding, which opens up opportunities to study dynamics and relaxation of interfacial chains in the future.

Acknowledgment. We thank Dr. Raj Ganguli at Air Force Research Laboratory for performing the XPS experiments. We acknowledge funding from NSF (DMR-0512156).

References and Notes

- (1) Brown, H. R. *Science* **1994**, *263*, 1411–1413.
- (2) Chaudhury, M. K.; Owen, M. J. *Langmuir* **1993**, *9*, 29–31.
- (3) Vorvolakos, K.; Chaudhury, M. K. *Langmuir* **2003**, *19*, 6778–6787.
- (4) Yurdumakan, B.; Nanjundiah, K.; Dhinojwala, A. *J. Phys. Chem. C* **2007**, *111*, 960–965.
- (5) Jackman, R. J.; Wilbur, J. L.; Whitesides, G. M. *Science* **1995**, *269*, 664–666.
- (6) Kumar, A.; Biebuyck, H. A.; Whitesides, G. M. *Langmuir* **1994**, *10*, 1498–1511.
- (7) Owen, M. J. *Surf. Coat. Int.* **1996**, *79*, 400–405.

- (8) Spilizewski, K. L.; Marchant, R. E.; Anderson, J. M.; Hiltner, A. *Biomaterials* **1987**, *8*, 12–17.
- (9) Shen, Y. R. *Nature* **1989**, *337*, 519–525.
- (10) Yurdumakan, B.; Harp, G. P.; Tsige, M.; Dhinojwala, A. *Langmuir* **2005**, *21*, 10316–10319.
- (11) Clancy, T. C.; Jang, J. H.; Dhinojwala, A.; Mattice, W. L. *J. Phys. Chem. B* **2001**, *105*, 11493–11497.
- (12) Schallamach, A. *Wear* **1963**, *6*, 375–382.
- (13) Nanjundiah, K.; Hsu, P. Y.; Dhinojwala, A. *J. Chem. Phys.* **2009**, *130*, 024702/1–7.
- (14) Johnson, K. L.; Kendall, K.; Roberts, A. D. *Proc. R. Soc. London, Ser. A* **1971**, *324*, 301–313.
- (15) Chaudhury, M. K.; Whitesides, G. M. *Langmuir* **1991**, *7*, 1013–1025.
- (16) Ahn, D.; Shull, K. R. *Macromolecules* **1996**, *29*, 4381–4390.
- (17) Smith, G. C. *Surface Analysis by Electron Spectroscopy: Measurement and Interpretation*; Plenum Press: New York, 1994.
- (18) Shen, Y. R. *The Principles of Nonlinear Optics*; John Wiley & Sons: New York, 1984.
- (19) Bain, C. D. *J. Chem. Soc., Faraday Trans.* **1995**, *91*, 1281–1296.
- (20) Gautam, K. S.; Schwab, A. D.; Dhinojwala, A.; Zhang, D.; Dougal, S. M.; Yeganeh, M. S. *Phys. Rev. Lett.* **2000**, *85*, 3854–3857.
- (21) Harp, G. P.; Gautam, K. S.; Dhinojwala, A. *J. Am. Chem. Soc.* **2002**, *124*, 7908–7909.
- (22) Harp, G. P.; Rangwalla, H.; Yeganeh, M. S.; Dhinojwala, A. *J. Am. Chem. Soc.* **2003**, *125*, 11283–11290.
- (23) Beamson, G.; Briggs, D. *High Resolution XPS of Organic Polymers: The Scienta ESCA300 Database*; John Wiley & Sons: New York, 1992.
- (24) Watanabe, N.; Yamamoto, H.; Wada, A.; Domen, K.; Hirose, C.; Ohtake, T.; Mino, N. *Spectrochim. Acta* **1994**, *50A*, 1529–1537.
- (25) Roland, C. M.; Santangelo, P. G. *J. Non-Cryst. Solids* **2002**, *307–310*, 835–841.
- (26) Deruelle, M.; Leger, L.; Tirrell, M. *Macromolecules* **1995**, *28*, 7419–7428.
- (27) Maeda, N.; Chen, N.; Tirrell, M.; Israelachvili, J. N. *Science* **2002**, *297*, 379–382.